JOURNAL OF MATERIALS SCIENCE 37 (2002) 127–132

High temperature deformation behavior of permanent casting AZ91 alloy with and without Sb addition

YUAN GUANGYIN, WANG QUDONG, DING WENJIANG
Institute of Foundry Engineering, College of Materials Science and Engineering, Shanghai Jiaotong University, Shanghai 200030, People's Republic of China
E-mail: gyyuan@mail1.sjtu.edu.cn

The elevated temperature deformation behavior of permanent cast magnesium alloy AZ91 with and without Sb addition has been investigated using slow strain rate ($5.0 \times 10^{-4}s^{-1}$) elevated temperature tensile and constant load creep testing at 150°C and 50 MPa. The alloy with 0.4 wt% Sb showed a higher elevated temperature tensile strength and creep resistance due to the formation of thermal stable Mg_3Sb_2 precipitates and a smaller microstructure as well as the suppressing of the discontinuous precipitation. Plastic deformation of AZ91 based alloys is determined by motion of dislocation in basal plane and non-basal slip systems. The dislocation motion in a slip system is influenced by temperature, precipitates and other lattice defects. Dislocations jog, grain boundaries and/or precipitates are considered as obstacles for moving dislocations. The $(01\bar{1}2)$ deformation twinning were founded in the creep process by TEM. Cross slip of dislocations was taken into account as the main softening mechanism for permanent cast AZ91 alloy during elevated temperature deformation process.

1. Introduction

Magnesium is a material offering high weight reduction potential when used as structural material because of its low density and acceptable strength properties. This is the main reason for significant increase in the use of magnesium components in the automobile industry in recent years [1, 2]. The most frequently used cast magnesium alloy is AZ91(Mg-9Al-0.8Zn-0.2Mn). However, its low creep resistance at temperature in excess of 120°C limited its further application [2, 3]. Our previous work [4] indicated the proper addition of antimony to AZ91 increased the mechanical properties at elevated temperature up to 200°C greatly. The present study was undertaken to investigate the high-temperature deformation behavior of AZ91 with Sb and without Sb, and the relationship between the microstructure and elevated temperature properties of AZ91 was also discussed. Specimens have been subjected to low strain rate tensile at temperatures in the range of 20–200°C and constant load creep testing at temperature of 150°C.

2. Experimental procedure

Flat tensile specimens of magnesium alloy AZ91 (designated as alloy 1) and AZ91 + 0.4 wt%Sb (designated as alloy 2) were permanent cast using procedures described in literature [4]. The compositions of the alloys tested by using inductively coupled plasma (ICP) are shown in Table I. Tensile specimens with a gauge section of 15 mm × 3.5 mm × 2 mm were cut by electric spark machining from the ingots. Before testing the specimens were heated at 420°C for 12 h (T4 solution heat treatment) followed by water quenching, then aged at 200°C for 8 h. Tensile tests at ambient and elevated temperature were carried out at the strain rate of $5 \times 10^{-3}s^{-1}$ and $5 \times 10^{-4}s^{-1}$ respectively. Constant-load creep tests were carried out in air at temperature of 150°C. Metallography investigation was carried out using optical microscopy, scanning electron microscopy (SEM) and transmission electron microscopy (TEM). The samples of TEM were prepared as follows: after mechanically thinning to 0.1 mm, the slice was punched into 3 mm diameter discs. The discs were jet-electropolished with a solution of $HClO_4$: butanol : methanol = 5:35:60 at −30°C and the voltage range was between 10–15 V; the resulting specimen was examined in a JEOL-2000EX transmission electron microscope equipped with a double-tilt holder and operating at 160 KV.

3. Results

3.1. Microstructure

As described by Sequeira *et al.* [5], the microstructure of permanent cast AZ91 consists of a bimodal distribution of α-Mg grains together with intergranular β-$Mg_{17}Al_{12}$. The general nature of the microstructure of alloy 1 is shown in Fig. 1. Antimony addition resulted in the modification of the morphology of β phase in the

TABLE I The chemical compositions of alloys studied (wt%)

Alloy code	Al	Zn	Mn	Cu	Ni	Fe	Si	Sb	Other	Mg	Grain size (μm)
Alloy 1	8.90	0.79	0.25	0.002	0.001	0.005	0.02	–	0.01	Bal.	115
Alloy 2	8.87	0.82	0.27	0.004	0.001	0.004	0.02	0.4	0.01	Bal.	80

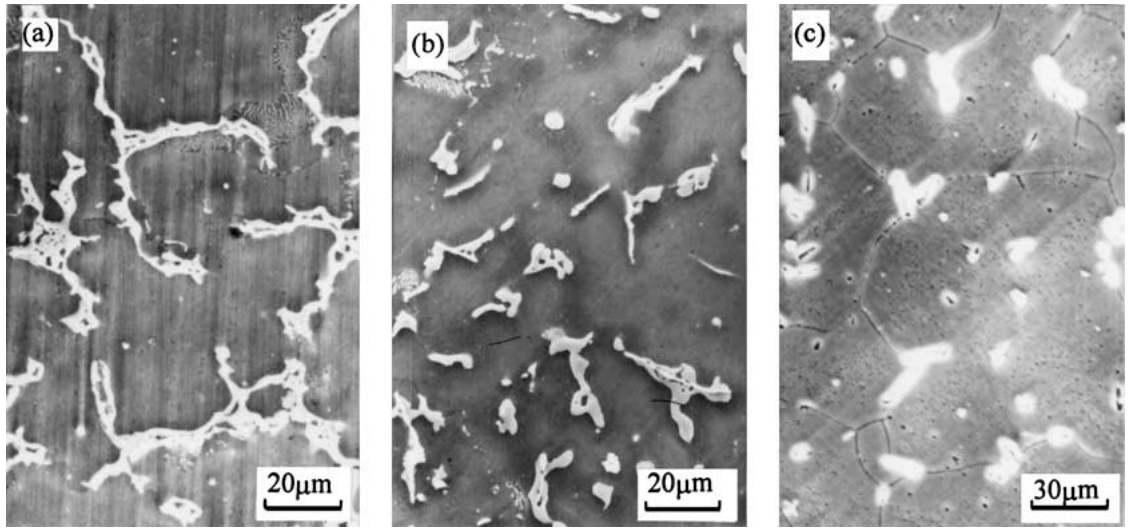

Figure 1 Microstructure of alloys studied (a) alloy 1—as-cast (b) alloy 2—as cast (c) alloy 2—T4 treated.

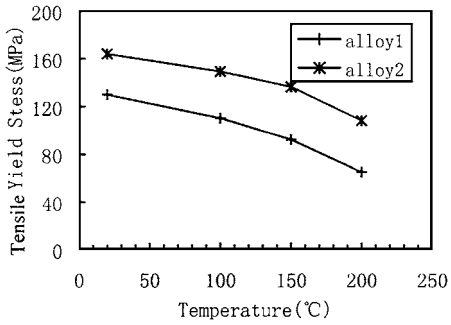

Figure 2 The yield strength at different temperatures for alloys studied.

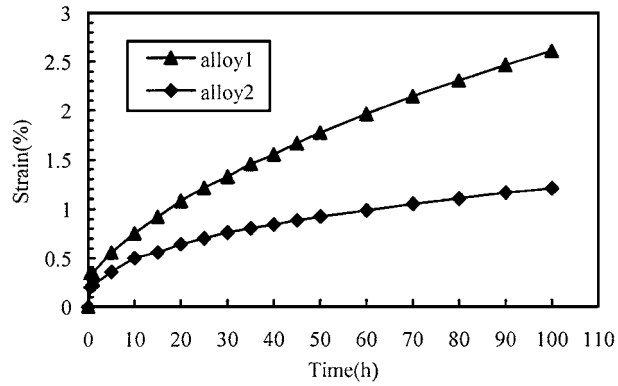

Figure 3 The creep curves of alloys for tests conducted at 50 Mpa and 150°C.

as-cast AZ91 alloy and reduction of the grain size. The average grain sizes of alloys in the T4 condition also listed in Table I. Fig. 1b shows the microstructure of alloy 2 containing 0.4 wt% of Sb. It can be seen that the β phase in this alloy is finer and its distribution is more uniform than that in AZ91. Furthermore, some rod-shaped dispersoids formed in the grain boundary areas with the Sb addition. These particles containing Sb were identified as Mg_3Sb_2, a hexagonal structure of $D5_2$ [4]. When the as-cast specimens of the alloys were homogenized at 420°C for 16 hours (T4 treatment), almost all of the β phase dissolved in the matrix, while the rod-shaped precipitates (Mg_3Sb_2) still existed in the matrix even after solution treatment at 420°C for 12 hours (see Fig. 1c) indicating the thermal stability of Mg_3Sb_2 phases.

3.2. Constant strain rate tensile tests

Fig. 2 shows the tensile yield strength at different temperature for specimens tested. It can be seen that Sb addition to AZ91 resulted in significant influence on tensile properties. In the range of ambient temperature to 200°C the yield strength was all increased greatly. Moreover, with the temperature increased, the yield strength of alloy 2 containing Sb decreased slowly compared to alloy 1 without Sb. This indicated that the thermal stability of AZ91 was increased significantly by Sb addition. Fine-grain strengthening and dispersion strengthening by Mg_3Sb_2 particles with Sb addition accounted for the improvement of mechanical properties of alloy 2 at both ambient and elevated temperature.

3.3. Constant load creep tests

Constant load creep tests were conducted at initial stresses of 50 Mpa at 150°C. The creep curves for 100 hours tests duration were plotted in Fig. 3 using microcomputer automatically monitored. From Fig. 3 it can be seen that the resistance to creep deformation increased with the antimony addition significantly. Table II listed the data of the total creep strains and minimum creep rates. As can be seen in Table II,

TABLE II Minimum creep rates and strain at 100 h for creep of two alloys with and without Sb addition at 150°C and 50 Mpa

Alloy code	Minimum creep rate (s^{-1})	Strain at 100 h (%)
Alloy 1	5.6×10^{-8}	2.4
Alloy 2	1.5×10^{-8}	1.2

the minimum creep rate (stable-state creep rate) is $5.6 \times 10^{-8}s^{-1}$, which is close to that reported in the literature [6] under the same testing condition. Whereas that of alloy 2 with 0.4%Sb decreased to $1.5 \times 10^{-8}s^{-1}$, about only quarter of that of the AZ91. The creep strain of alloy 2 within the same testing time is also one half lower than that of the Sb-free one correspondingly.

3.4. Microcharacterization of high temperature deformation behavior

3.4.1. Dislocations morphology

Figs 4 and 5 are TEM-micrographs taken from ambient temperature tensile testing (at the low strain rate of $5 \times 10^{-3}s^{-1}$) ruptured specimens of alloy 1 (AZ91). The TEM approach was carried out as literature [7].

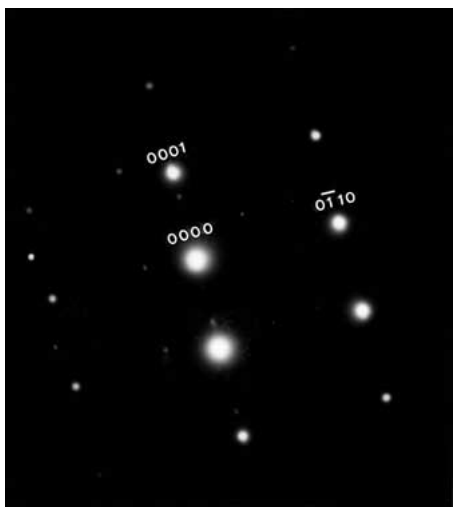

Figure 4 Electron diffraction pattern taken from tensile rupture specimen of alloy 2 along Zone axis $\langle 2\bar{1}\bar{1}0\rangle$.

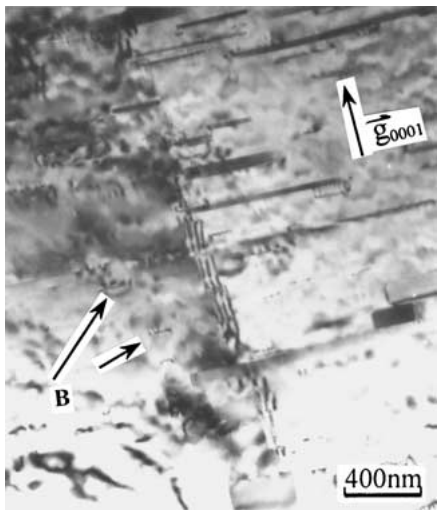

Figure 5 Bright field TEM micrograph taken from tensile ruptured specimen of alloy T2 along zone axis $\langle 2\bar{1}\bar{1}0\rangle$; B—basal dislocation.

The samples were titled into zone axes related to basal zones parallel to the incident electron beam, such as $\langle 2\bar{1}\bar{1}0\rangle$, with these zone axes, dislocation on basal zones should appear straight and parallel, while the orientations of basal planes can be obtained from the diffraction pattern. According to this procedure only basal (B) dislocation was observed in the sample of alloy 1 at ambient temperature tensile, as shown in Fig. 5. A lot of fine flake-shape continuous precipitates ($Mg_{17}Al_{12}$) distributed on the basal planes. During room temperature tensile deformation process, these precipitates acted as the obstacles of the dislocation glide. However, in the high temperature tensile samples, both basal and non-basal (NB) dislocations were observed, as shown in Fig. 6. Similar non-basal dislocations were also observed in elevated temperature crept samples of alloy 1. This shows that the dislocations on different slip plane were activated by a cross-slip process during high temperature deformation. The dislocations on different slip plane intercrossed resulting in the formation of some dislocation jogs (see Fig. 6).

The dislocation structures in the creep ruptured specimens containing Sb as shown in Fig. 7. It can be seen that a high concentration of creep produced dislocations distributed around the Sb-rich precipitates. This shows the hindering of dislocation movement by dispersoids and formation of dislocation tangles during creep process.

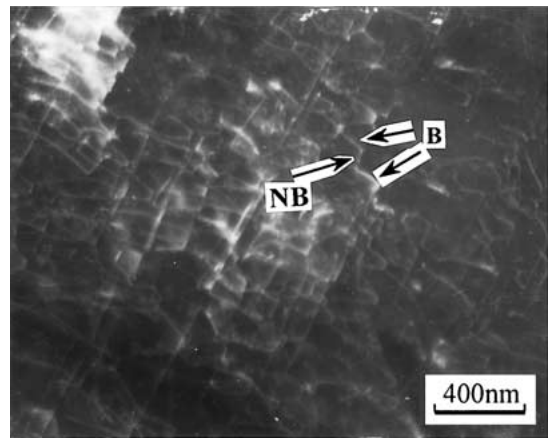

Figure 6 Dislocations in tensile fracture specimen of alloy 1 at 200°C. B—basal dislocation; NB—non-basal dislocation.

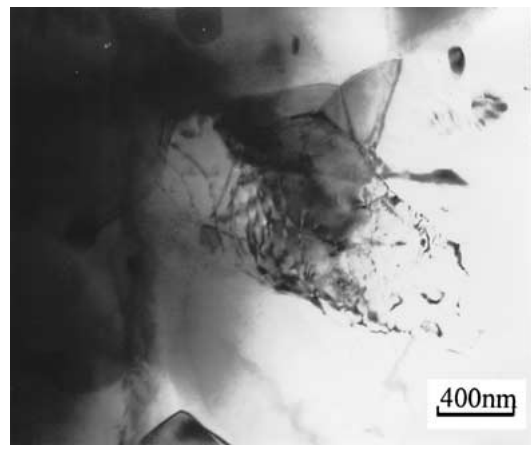

Figure 7 Dislocations in tensile fracture specimen of alloy 2 at 200°C.

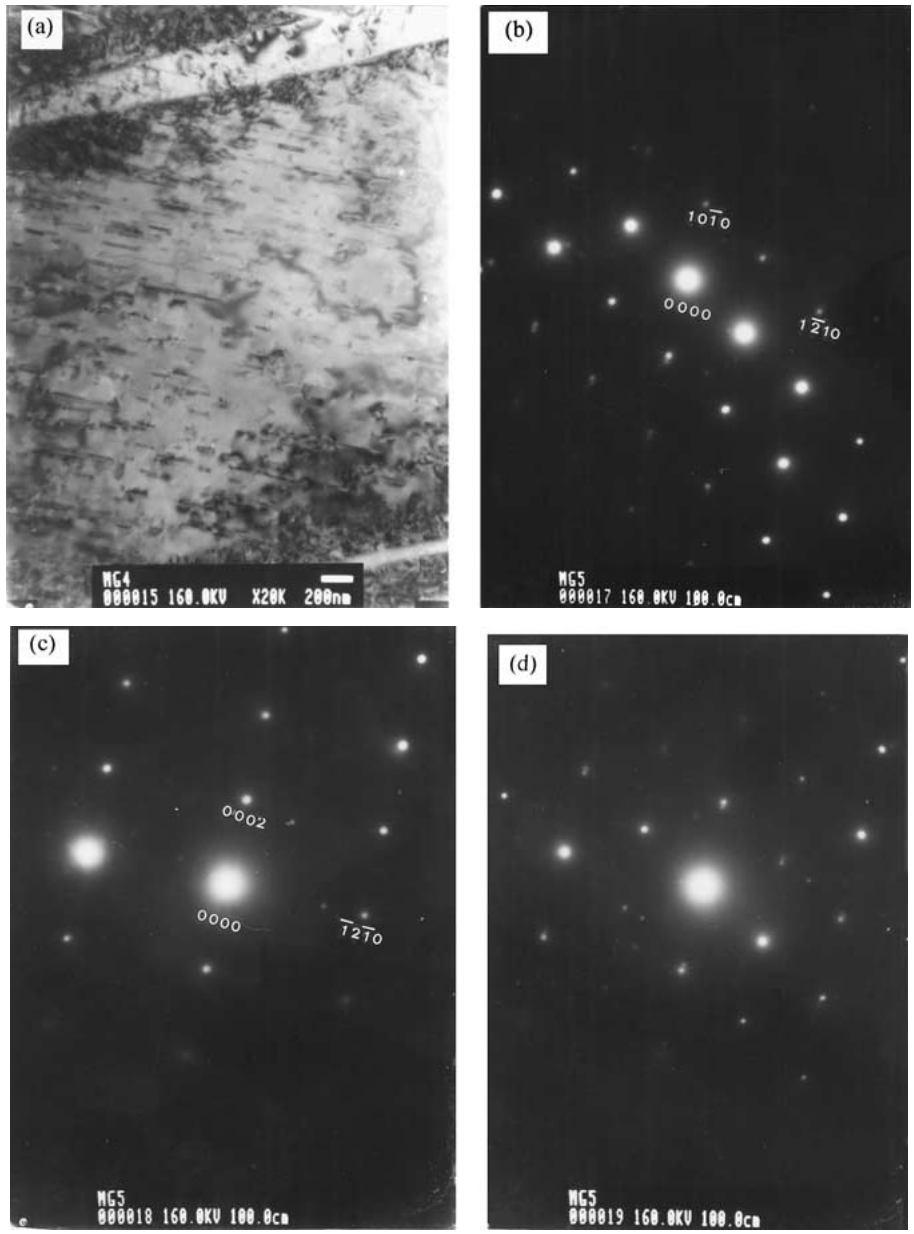

Figure 8 Twin morphology and its identification in alloy 2 (a) twin morphology; (b) electron diffraction pattern (EDP) taken from the matrix along zone axis [0001]; (c) EDP from the twin along zone axis [$10\bar{1}0$]; (d) the composite diffraction pattern of both Fig. 8b and c.

3.4.2. Twinning

Observations on polished surface of alloys after creep indicated twinning was also occurred. Twinning is an athermal shear deformation process involving mirrored movement of several atomic layers at small fault vectors. For hexagonal magnesium twinning is a significant mode of deformation. In the alloy 2 the $(01\bar{1}2)$ twin has been observed. Fig. 8 shows the morphology of the twin in alloy 2 after elevated temperature creep deformation. It was identified by TEM and the transformation matrix of crystallographic plane was calculated as the following:

$$T_{10\bar{1}2} = \begin{bmatrix} \overline{0.064} & 0.468 & 0.532 \\ 0 & \bar{1} & 0 \\ 1.873 & 0.936 & 0.064 \end{bmatrix}$$

By applying the above transformation matrix, the indices of crystallographic plane was calculated as following:

$$T_{10\bar{1}2} \cdot \begin{bmatrix} 1 \\ \bar{2} \\ 0 \end{bmatrix}_M = \begin{bmatrix} \bar{1} \\ 2 \\ 0 \end{bmatrix}_T$$

The electron diffraction patterns of twin were identified as Fig. 8b and c. The Fig. 8d was the composite diffraction pattern of both Fig. 8b and c.

3.4.3. Fractographic observation

During both creep and elevated temperature tensile testing, considerable growth of cavities occurred and final failure occurred by the interlinkage and propagation of these cavities. Fig. 9 is the SEM morphology, performed on longitudinal cross sections of gage portions close to fractography creep ruptured specimens tested at 150°C and 50 Mpa, revealed the general differences in the appearance of the fracture in alloy 1 (AZ91) vs. the Sb-containing alloy 2. From Fig. 9a it can be seen that the grains of alloy 1 (AZ91) were prolonged

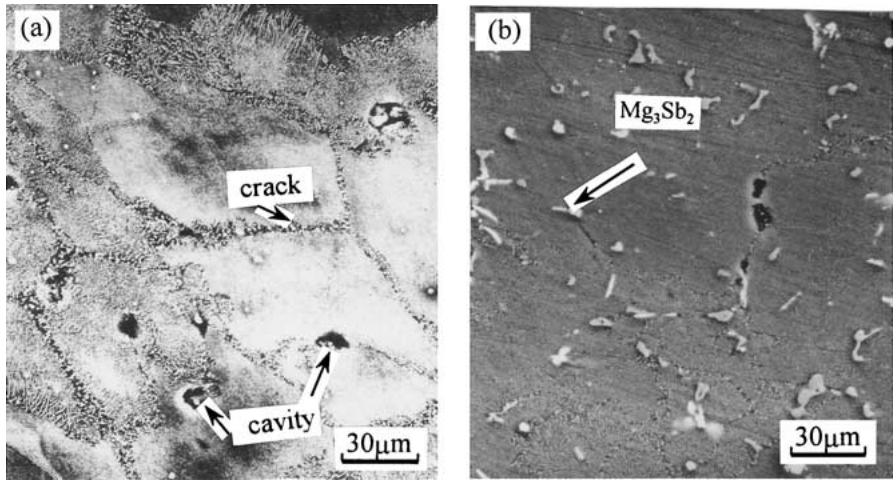

Figure 9 SEM micrographs of longitudinal cross section near the fracture surface (a) alloy 1 (b) alloy 2.

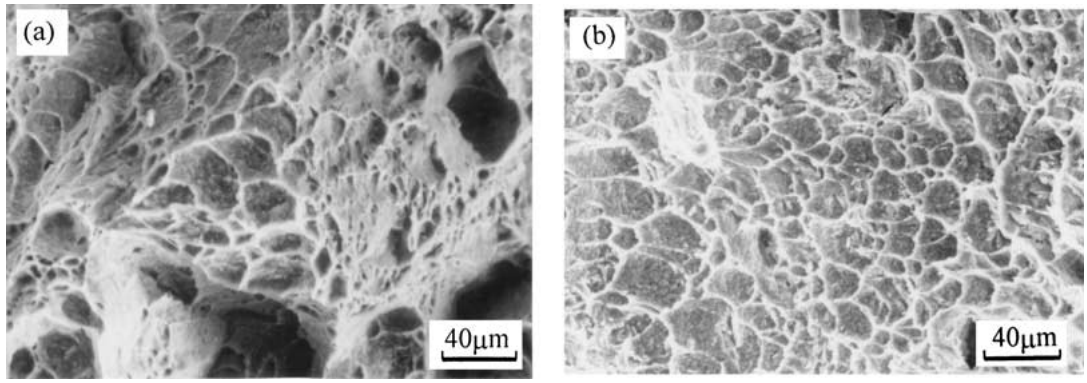

Figure 10 Fractography of creep ruptured specimens (a) alloy 1 (b) alloy 2.

obvious and considerable cavities developed during creep deformation. The micro-cracks initiated preferentially in the interface between lamellae discontinuous precipitates and the α-Mg grains. Some wedge-shaped cavities existed at triple points along grain boundaries perpendicular to the stress axis. The appearance of the cracks suggested initial cracks propagation and then cracks widening as either adjacent boundaries slide and/or the adjacent matrix deforms. In comparison with alloy 1, no obvious prolonged grain can be found in creep ruptured specimen of alloy 2 which containing 0.4%Sb, and only few cavities existed separately at the grain boundaries, as shown in Fig. 9b. Since the lamellae discontinuous precipitates were suppressed by Sb addition (see Fig. 9b), the number of micro-crack source consequently reduced. Moreover, the thermal stable dispersoids (Mg_3Sb_2) which mainly distributed along grain boundarie should block the further propagation and development of cracks.

Fig. 10 shows the fractography of specimens after elevated temperature creep test until specimens failed. Large and deep dimples about 30 μm in diameter can be seen on the alloy 1 specimen indicating ductile fracture feature (see Fig. 10a). As shown in Fig. 10b, dimples can also be observed in the alloy 2. The dimple size is less than 20 μm, which is much smaller than that of alloy 1, due to the smaller grain size and the presence of dispersed phases. Compared with the alloy 1, the alloy 2 shows a relatively brittle feature. This conforms to the describe above about the deformation morphology characteristic of alloys. No clear debonding between the dispersoids and matrix can be seen (Fig. 10b), which indicating the Mg_3Sb_2 dispersoids is well bounded with the matrix.

4. Discussion

4.1. Influence of Sb addition on creep resistance of AZ91

The previous investigation [3] proposed that the main reason for the poor creep properties of AZ91 is that the intergranular β-$Mg_{17}Al_{12}$ phase softens at elevated temperatures and this results in excessive deformation in the grain boundary regions. Results obtained in the present work are agree with this hypothesis. The body-centered cubic (b.c.c.) structure of $Mg_{17}Al_{12}$ is incompatible with the h.c.p structure of magnesium matrix, which leads to the fragility of the Mg/$Mg_{17}Al_{12}$ interface. So the microcrack is prone to initiate in the Mg/$Mg_{17}Al_{12}$ interface under the stress (see Fig. 9a). In addition, the study [8] showed that in Mg-Al alloys the sliding of grain boundaries is an important deformation mechanism. The presence of many lamellae discontinuous precipitates in the vicinity of grain boundaries provided more surfaces on which sliding took place, as shown in Fig. 9a. Therefore, to achieve markedly improved creep resistance of AZ91, it demands a method for making the alloy containing continuous precipitates within the grain to impede dislocation motion and producing thermal stable intergranular

phases to reduce grain boundary sliding. It seems a feasible way to try to suppress the discontinuous precipitation that occurs at grain boundaries from the aging process. This has a two-fold benefit, it increases the volume of matrix available for continuous precipitation and it may decrease the amount of grain boundary sliding and deformation. One effective means of altering the precipitation behavior is the addition of some surface active elements to AZ91 [9]. In present work, we have observed that the proper addition of Sb suppressed the discontinuous precipitates effectively, also resulted in the refinement of microstructure and the formation of effective grain boundary phases to block sliding.

4.2. Deformation mechanism for permanent casting AZ91

At ambient temperature, deformation mechanism of alloy AZ91 is determined by the dislocation glide on basal plane which has been verified by TEM study. Grain boundaries and/or precipitates are considered as obstacles for moving dislocations, as shown in Fig. 5. As temperature increased, the deformation mechanism of alloy AZ91 changed. Both basal and non-basal dislocations were observed in the elevated temperature deformation samples. Precipitates and dispersoids acted as the obstacles of the dislocation movement, see Fig. 5. Therefore, the dislocation motion in a slip system is influenced by temperature and precipitates for magnesium alloy AZ91.

According to previous studies performed on pure magnesium in the temperature of 150°C [10, 11], the dislocation glide on basal planes controls creep behavior. Since magnesium has only three active slip systems exist and therefore the fracture is brittle type. The relatively large deformation before fracture obtained with alloy 1 during creep seems to contradict the basal dislocation glide controlled creep view. TEM studies performed on crept specimens observed some mobile dislocations on non-basal planes, which suggested cross slip occurred during creep process. Also, the $(01\bar{1}2)$ twining would take place if the basal plane is unfavorably oriented. Therefore, cross slip should be the main softening mechanism for permanent cast AZ91 in the creep of temperature of 150°C.

4.3. $(01\bar{1}2)$ Twining mechanism

Although the twinning mechanism has been studied for many years, it is not yet completely understood. As for the formation of $(01\bar{1}2)$ twin in AZ91 based alloys during high temperature creep deformation, it may be a result of slip. Because dislocations arrays should lead to stress concentrations and which can then cause the nucleation of twins. This twin grows under stress and lattice dislocations can interact with grain boundaries during deformation of alloys. The result of this reaction may be the $(01\bar{1}2)$ twin.

5. Conclusions

The effects of Sb addition on the high temperature deformation behavior and fracture mechanism in AZ91 alloy can be summarized from the present investigation results as follows:

1. Small amount (0.4 wt%) of Sb addition to AZ91 modified the morphology of $Mg_{17}Al_{12}$ phase, refined the microstructure and resulted in the formation of rod-like Mg_3Sb_2 particles as grain boundaries strengthening phase.
2. The addition of 0.4 wt%Sb in AZ91 effectively increased tensile strength at elevated temperature and creep resistance. In particularly, the minimum creep rate of the alloy with 0.4%Sb significantly reduced to only quarter of that of the Sb-free alloy under the creep condition of 150°C/50 Mpa.
3. The creep microcracks initiated preferentially in the interface between discontinuous precipitation and the α-Mg grains. The appearance of the cracks suggested initial cracks propagation and then cracks widening as either adjacent boundaries slide and/or the adjacent matrix deforms. The higher high-temperature deformation resistant of alloy containing Sb attributed to the suppression of discontinuous precipitation and formation of effective grain boundaries phase.
4. Cross slip is considered to be the main softening mechanism for permanent cast AZ91 in the creep of temperature of 150°C.
5. $(01\bar{1}2)$ twinning was observed in AZ91 alloy during creep and it may be the reaction result of lattice dislocation interacting with grain boundaries.

Acknowledgements

Thanks are due to Dr. Shen Guangjun (Analysis and Testing center, Southeast University, P. R. China) for the technical advice and assistance in TEM research work, and to Prof. Sun Yangshan (Dep. Mater. Sci. & Eng., Southeast University. P. R. China) for fruitful discussion.

References

1. ZHAN ZHANG, ALAIN COUTURE and A. LUO, *Scripta Materialia* **39** (1998) 45.
2. A. LUO and M. O. PEKGULERYUZ, *J. Mater. Sci.* **29** (1994) 5259.
3. P. HUMBLE, *Materials Forium* **21** (1997) 45.
4. YUAN GUANGYIN, SUN YANGSHAN and ZHANG WEIMING, *J. Mater. Sci. Lett.* **18** (1999) 2055.
5. W. P. SEQUEIRA, M. T. MURRAY and G. L. DUNLOP, in Proc. 3rd International Magnesium Conference, edited by G. W. Lorimer (Institute of Materials, Manchester, 1997) p. 63.
6. M. DARGUSCH, M. HISA, C. H. CACERES and G. L. DUNLOP, in Proc. 3rd International Magnesium Conference, edited by G. W. Lorimer (Institute of Materials, Manchester, 1997) p. 153.
7. M. REGEV, E. AGHION, S. BERGER, *et al.*, *Mater. Sci. Eng.* **A257** (1998) 349.
8. C. S. ROBERTS, in "Magnesium and its Alloys" (Wiley, New York, 1960) p. 102.
9. C. J. BETTLES, P. HUMBLE and J. F. NIE, in Proc. 3rd International Magnesium Conference, edited by G. W. Lorimer (Institute of Materials, Manchester, 1997) p. 403.
10. W. J. McG. Tegart, *Acta Metall.* **9** (1961) 614.
11. S. S. VAGARLI and T. G. LANGDON, *ibid.* **29** (1981) 1969.

Received 1 November 2000
and accepted 13 August 2001